Desalination and Water Treatment
www.deswater.com
doi: 10.1080/19443994.2013.769728

51 (2013) 6743–6754
October

Taylor & Francis
Taylor & Francis Group

Studies on fluoride adsorption by apatitic tricalcium phosphate (ATCP) from aqueous solution

M. Mourabet*, A. El Rhilassi, M. Bennani-Ziatni, R. El Hamri, A. Taitai

Faculty of Sciences, Team Chemistry and Valorization of Inorganic Phosphates, Department of Chemistry, Kenitra, BP133, Morocco
Tel. +212 6 02 26 82 83; email: mrab.et@hotmail.com

Received 23 March 2012; Accepted 20 January 2013

ABSTRACT

The present study was conducted to evaluate the feasibility of apatitic tricalcium phosphate (ATCP) for fluoride adsorption from aqueous solutions. The adsorbent was characterized using X-ray diffraction and scanning electron microscope with energy dispersive X-ray analysis. Batch adsorption studies were performed as function of contact time, initial fluoride concentration, temperature, adsorbent dose, pH, and influence of competing anions. Fluoride adsorption kinetics was well fitted by pseudo-second-order model. The maximum sorption capacity of ATCP for fluoride removal was found to be 15.42 mg g^{-1} at 313 K. Thermodynamic parameters viz. ΔG°, ΔH°, and ΔS° were calculated indicating that the adsorption process was spontaneous and endothermic. The fluoride adsorption was well explained using Langmuir Freundlich, Temkin and Dubinin–Radushkevick models. Fluoride adsorption was influenced by the presence of HCO_3^- ions. It was observed that at pH = 12.75 around 88% desorption efficiency was found. Results from this study demonstrated potential utility of ATCP that could be developed into a viable technology for fluoride removal from aqueous solution.

Keywords: Apatitic tricalcium phosphate; Fluoride; Adsorption isotherms; Adsorption kinetics

1. Introduction

Fluoride contamination of drinking water is a worldwide problem, and excess intake of fluoride can cause harmful effects such as dental/skeletal fluorosis, fetal cerebral function, neurotransmitters, etc. Taking health effects into consideration, the World Health Organization has set a guideline value of 1.5 mg L^{-1} [1] as the maximum permissible level of fluoride in drinking water. Many countries have regions where water contains fluoride concentration more than the prescribed limit. The fluoride occurs in nature mainly as sellaite (MgF_2), fluorspar (CaF_2), cryolite (Na_3AlF_6), and fluorapatite ($Ca_5(PO_4)_3F$). These fluoride minerals are nearly insoluble in water. Hence, fluoride will be present in groundwater only when conditions favor their dissolution or high fluoride containing effluents are discharged to the water bodies from the industries. High fluoride concentrations in groundwater, up to more than 30 mg L^{-1}, have been observed widely in many parts of the world [2].

Considering the serious health effects of fluoride, several technologies, including precipitation, adsorption, ion exchange, membrane separation, and electrodialysis were developed and evaluated for

---

*Corresponding author.

fluoride removal. Among these methods, adsorption seems to be the most attractive method because of its high efficiency and easy handling nature. About 100 adsorbents have been successfully exploited for the removal of fluoride [3], including activated carbon [4], low cost materials [5], activated alumina [6], waste mud [7], montmorillonite [8], some geomaterials [9], and other materials.

Several studies have shown interest in the use of calcium phosphate and various apatite materials [10] in fluoride removal: synthetic hydroxyapatite at nanoscale [11], glass-derived hydroxyapatite [12], hydroxyapatite [13], and brushite [14]. Calcium phosphates, especially apatites, present remarkable interest; their availability structure, ionic exchange property, and adsorption affinity have conferred to this material to attract more attention. In addition, this material can be efficient matrices of water purification.

In the present study, the sorption feasibility of apatitic tricalcium phosphate (ATCP), which is a solid with atomic ratio of Ca/P equal to 1.5, was assessed for fluoride removal from aqueous solution. The physical and chemical characterization of ATCP by X-ray diffraction (XRD), scanning electron microscope (SEM), and energy dispersive X-ray (EDX) were conducted and further the potential of the ATCP was evaluated for fluoride removal. Defluoridation studies were conducted under various experimental conditions, such as pH, contact time, initial fluoride concentrations, temperature, and the presence of competing anions. The data from the experiments were fitted with different models to identify the adsorption mechanism. The results have been thoroughly discussed which would help in the better understanding of defluoridation mechanism by ATCP.

2. Materials and methods

2.1. Adsorbent

The ATCP ($Ca_9(HPO_4)(PO_4)_5(OH)$) powders were prepared by an aqueous double decomposition of the salts of calcium and of phosphate [15].

SEM and EDX analysis were performed using an FEI Tecanai G2 (Philips). An XRD pattern was analyzed using X'Pert PRO (Germany) X-ray diffractometer with Cu Kα radiation.

2.2. Adsorption studies

Adsorption studies of fluoride were investigated by batch experiments. All batch experiments were carried out in 150 mL glass bottle. For preparing the samples, 0.2 g of ATCP was added in 50 mL of fluoride solutions. The mixture was agitated at 400 rpm. The solution was then filtered and the residual fluoride ion concentration was analyzed electrochemically with a fluoride ion-selective electrode (Orion, USA) by the use of total ionic strength adjustment buffer (TISAB) solution.

The specific amount q_e ($mg\,g^{-1}$) of fluoride adsorbed was calculated by following expression:

$$q_e = \frac{(C_o - C_e)V}{m} \tag{1}$$

where q_e is the fluoride adsorbed ($mg\,g^{-1}$); C_o, initial concentration of fluoride ($mg\,L^{-1}$); C_e, concentration of fluoride in solution at equilibrium time; V, solution volume (L); m, adsorbent dosage (g).

Adsorption isotherm was studied at three different temperatures, 298, 303, and 313 K on fluoride solutions with varying concentrations from 30 to 60 $mg\,L^{-1}$ and at initial solution pH (6.8–6.9)

Kinetic studies were carried at three different initial fluoride concentrations (30, 50, and 40 $mg\,L^{-1}$), three different temperatures (293, 303, and 313 K), and at contact time (1, 2, 3, 4, 5, 6, 7, 8, 9, 10, 20, 30, 40, 60, 90, 120, and 180 min).

2.3. Determination of model parameters

The parameters of models were determined using a nonlinear regression. Nonlinear analysis method gives a possibility to avoid errors because isotherm and kinetic models are described by nonlinear expressions and there is no necessity to alter function, thus error distribution would not change. This procedure gives true and unfailing model parameters because the nonlinear analysis is conducted on the same abscissa and ordinate. Thus, it is more suitable to determine the model parameters by this method. The coefficient of determination R^2, was used to test the best-fitting model to the experimental data:

$$R^2 = 1 - \frac{SS_{resid}}{SS_{total}} \tag{2}$$

where SS_{resid} is the sum of the squared residuals from the regression and SS_{total} is the sum of the squared differences from the mean of the dependent variable.

3. Results and discussion

3.1. Characterization of apatitic tricalcium phosphate

Fig. 1 shows the XRD patterns of the ATCP before and after adsorption of fluoride ions. The main peaks

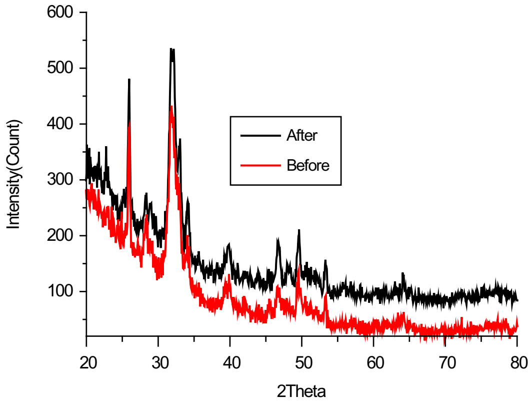

Fig. 1. XRD of apatitic tricalcium phosphate before and after adsorption of fluoride.

are characteristic peaks of ATCP. The ATCP can be identified as a poorly crystalline material. There is no marked change in the XRD pattern of ATCP after treatment with fluoride; this can be explained by ion exchange.

The surface condition and the existence of fluoride onto ATCP were confirmed by the SEM with EDX analysis. Fig. 2(a) and (b) shows the SEM images before and after fluoride adsorption with ATCP. The changes in the surface morphology of ATCP before and after fluoride treatment indicate fluoride adsorption on ATCP. The EDX spectrum of ATCP confirms the elements present in it and is shown in Fig. 2(c). The presence of a fluoride peak in the EDX spectra of fluoride-adsorbed ATCP confirms the fluoride adsorption onto ATCP which is shown in Fig. 2(d).

3.2. Effect of adsorbent dosage

The percent removal varies with different dosages of sorbent, viz. 0.05, 0.1, 0.15, 0.2, 0.30, and 0.4 g and have been studied to ascertain the effect of dosage with initial concentration 30 mg L^{1}, contact time 90 min, natural solution pH, and temperature 298 K. The sorption capacities of ATCP for fluoride ions decreased with the increase of the sorbent dosage from 0.05 to 0.4 g of ATCP. Fig. 3 shows the fluoride ions sorption capacities and percentage removal vs. sorbent dosage. The maximum sorption capacity was found by using 0.05 g of ATCP. The percentage removal of fluoride significantly increases with increase in sorbent dosage, which is obvious because of the increase in the number of active sites as the dosage increases. Furthermore, the adsorption capacity (q_e, mg g^{-1}) value was decreased for a fixed fluoride concentration with the increase of dose. The maximum fluoride removal of 96.37% was obtained using 0.4 g of ATCP.

3.3. Effect of initial pH

Influence of pH on fluoride adsorption by ATCP was investigated and the data are shown in Fig. 4. Fluoride adsorption by ATCP is sensitive to pH variations. It can be seen that the increase in the pH value decreases the adsorption capacity of ATCP (at pH 4 and 11, $q_e = 6.61$, and 4.303 mg g^{-1}, respectively). It is in relation with the surface charge of ATCP. The surface of ATCP is negatively charged when pH value is above the $\mathrm{pH_{PZC}} = 6$(zero point charge) [16] and positive charged when pH value is below the $\mathrm{pH_{PZC}}$. According to several authors, the exchange $\mathrm{OH^-}$ with fluoride may play an important role in fluoride removal.

Maliyekkal et al. [17] reported that the possible reaction mechanism for adsorption of fluoride onto magnesia-amended activated alumina (MAAA) can be hypothesized as below:

$$\mathrm{MgO} + \mathrm{H_2O} \rightarrow \mathrm{Mg(OH)_2} \tag{3}$$

$$\mathrm{Mg(OH)_2} + \mathrm{F^-} \leftrightarrow \mathrm{Mg(OH)_{2-y}F_y} \tag{4}$$

Zhang et al. [18] found at pH = 7.0, fluoride ions are predominantly adsorbed by the following surface-exchange reactions:

$$\begin{aligned}&\text{Graphene } \mathrm{OH_2^+}(\text{surf}) + \mathrm{F^-}\\ &\quad = \text{Graphene F}(\text{surf}) + \mathrm{H_2O}\end{aligned} \tag{5}$$

$$\begin{aligned}&\text{Graphene OH (surf)} + \mathrm{F^-}\\ &\quad = \text{Graphene F (surf)} + \mathrm{OH^-}\end{aligned} \tag{6}$$

Reyes and Rios [19] indicated that the chemical sorption of fluoride may be explained by the following reaction:

$$\mathrm{Ca_5(PO_4)_3OH} + \mathrm{F^-} \rightleftharpoons \mathrm{Ca_5(PO_4)_3F} + \mathrm{OH^-} \tag{7}$$

Chen et al. [20] proposed that the mechanism involved in the fluoride adsorption process using Al/Fe dispersed in porous granular ceramics can be described by the following equations, where M is $\mathrm{Al^{3+}}$ and $\mathrm{Fe^{3+}}$ bound to porous granular ceramics:

$$\mathrm{MCl_s} + \mathrm{H_2O} \rightarrow \mathrm{MOH_s} + \mathrm{H^+} + \mathrm{Cl^-} \tag{8}$$

$$\mathrm{MOH_{(s)}} + \mathrm{H_3O^+} + \mathrm{F^-} \rightarrow \mathrm{MOH_2^+} \cdots \mathrm{F^-_{(s)}} + \mathrm{H_2O} \tag{9}$$

$$\mathrm{MOH} + \mathrm{H_3O^+} \rightarrow \mathrm{M^+} \cdots \mathrm{F^-_{(s)}} + 2\mathrm{H_2O} \tag{10}$$

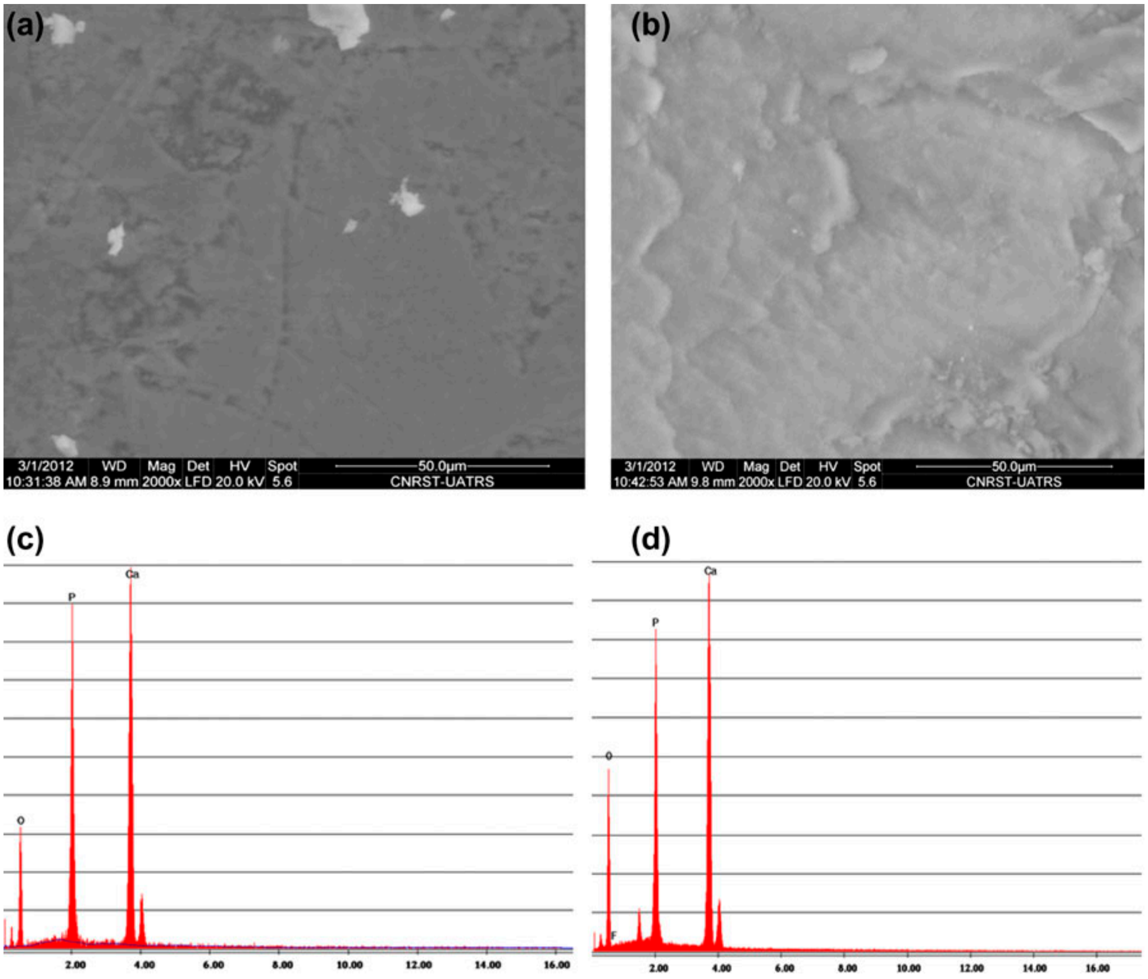

Fig. 2. SEM images of (a) ATCP and (b) fluoride-adsorbed ATCP and EDX spectra of (c) ATCP and (d) fluoride-adsorbed ATCP.

Sujana et al. [21] investigated the adsorption of fluoride on Bauxite and confirmed that the mechanism of fluoride adsorption can be represented as

$$\equiv \mathrm{MOH}_2^+ + \mathrm{F}^- \leftrightarrow \equiv \mathrm{MF} + \mathrm{H_2O} \quad (11)$$

$$\equiv \mathrm{MOH} + \mathrm{H}^+ + \mathrm{F}^- \leftrightarrow \equiv \mathrm{MF} + \mathrm{H_2O} \quad (12)$$

$$\equiv \mathrm{MOH} + \mathrm{F}^- \leftrightarrow \equiv \mathrm{MF} + \mathrm{OH}^- \quad (13)$$

where $M = \mathrm{Al}$, Fe, Si or Ti.

Finally, Ma et al. [22] explained that the specific adsorption of anions on HO-CaBen (hydroxyl Ca-bentonite) occurs via ligand exchange reactions, in which hydroxyl surface groups are replaced by the ions to be adsorbed and the adsorption process can be described by the following reactions:

$$\equiv \mathrm{MOH} + \mathrm{H}^+ \leftrightarrow \equiv \mathrm{MOH}_2^+ \quad (14)$$

$$\equiv \mathrm{MOH}_2^+ + \mathrm{F}^- \leftrightarrow \equiv \mathrm{MOH}_2 - \mathrm{F} \quad (15)$$

$$\equiv \mathrm{MOH}_2^+ + \mathrm{F}^- \leftrightarrow \equiv \mathrm{MF} + \mathrm{H_2O} \quad (16)$$

$$2[\equiv \mathrm{MOH}] + 2\mathrm{F}^- \leftrightarrow \equiv \mathrm{MOF} \equiv \mathrm{MF} + \mathrm{H_2O} \quad (17)$$

where M represents Ca and F represents the anion.

Hence, in the adsorption process, fluoride ions could replace hydroxyl ions (OH^-) on the surfaces of ATCP (P–OH P–F). Additionally, below point of zero charge where ATCP is positively charged, electrostatic attraction could occur between negatively charged fluoride ions and positively charged surfaces of ATCP $(\mathrm{P} - \mathrm{OH}_2^+\ \mathrm{F}^-)$.

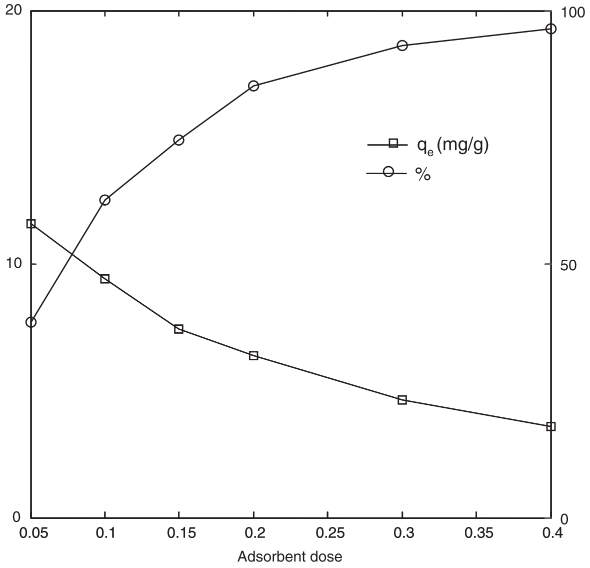

Fig. 3. Effect of adsorbent dose (initial concentration 30 mg L^{1}, contact time 90 min, temperature 298 K, and initial solution pH (6.8–6.9)).

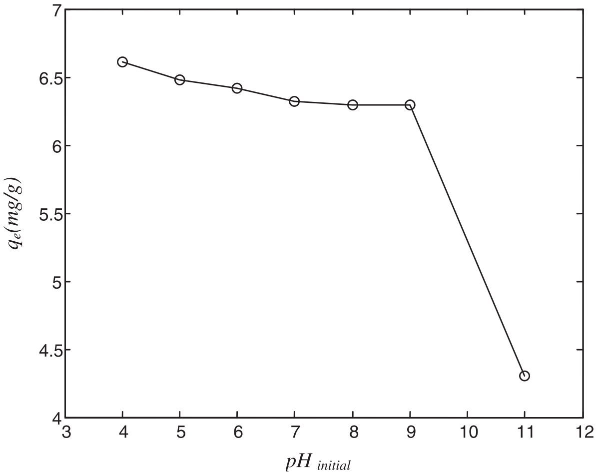

Fig. 4. Effect of initial pH (adsorbent dose 0.2 g, initial concentration 30 mg L^{1}, contact time 90 min, and temperature 298 K).

3.4. Adsorption isotherm

Many adsorption isotherm models have been successfully applied to describe the adsorption process. In this study, four different isotherm models were tested: the Langmuir [23], the Freundlich [24], the Temkin [25], and the Dubinin–Radushkevick (D–R) [26] models.

The Langmuir isotherm was developed on the assumption that the adsorption process will only take place at specific homogenous sites within the adsorbent surface with uniform distribution of energy level. Once the adsorbate is attached on the site, no further adsorption can take place at that site, which concluded that the adsorption process is monolayer in nature.

The nonlinear form of the Langmuir equation can be described by

$$q_e = \frac{Q_m b C_e}{1 + bC_e} \tag{18}$$

where C_e (mg L^{1}) is the equilibrium concentration of the adsorbate, q_e (mg g^{1}) is the amount of adsorbate per unit mass of adsorbent, Q_m (mg g^{1}) and b (L mg^{1}) are Langmuir constants related to sorption capacity and rate of sorption, respectively. The maximum adsorption capacities of F, Q_m, and constant related to the binding energy of the sorption system, b are calculated (Fig. 5) and listed in Table 3. The sorption capacity, Q_m, which is a measure of the maximum adsorption capacity corresponding to complete monolayer coverage found to be 15.42 mg g^{-1} for the experiments carried out at 40°C.

Table 1 lists a comparison of adsorption capacity of ATCP with those obtained in the literature for the adsorption of fluoride. The adsorption capacity of ATCP for fluoride was 13.54 mg g^{-1} at 298 K. The calculated adsorption capacities exhibit a good capacity for fluoride sorption from aqueous solutions. The feasibility of the isotherm was tested by calculating the dimensionless constant separation factor or equilibrium parameter R_L [32].

$$R_L = 1/1 + b\ C_0 \tag{19}$$

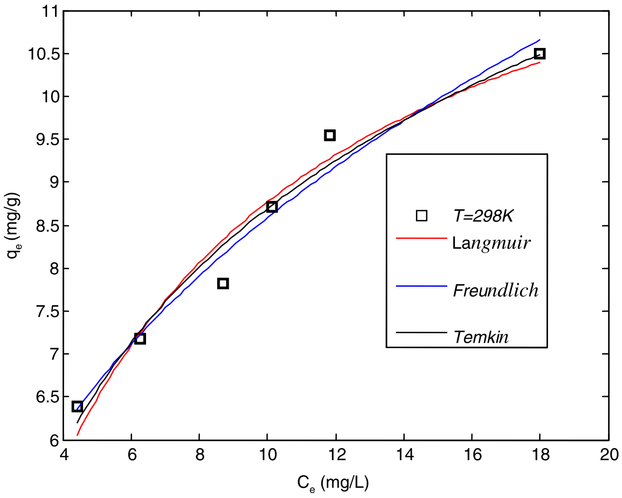

Fig. 5. Isotherms obtained using the nonlinear method for the adsorption of fluoride onto ATCP at a temperature of 298 K. (adsorbent dose 0.2 g, initial concentration 30–60 mg L^{1}, contact time 90 min, and pH (6.8–6.9)).

Table 1
Comparison of adsorption capacity of apatitic tricalcium phosphate with those adsorbents

Adsorbent	pHpzc	Q_m(mg g^{-1})	Concentration range(mg L^1)	Contact time	pH	Ref.
Brushite	6.2	6.59	20–50	60 min	6.8–6.9	[14]
Zirconium–iron oxide	–	9.8	10	10 h	7	[27]
Titanium/chitosan	–	7.20	–	24 h	7	[28]
Magnesia-amended activated alumina	8.6	10.12	5–150	3 h	6.5–7	[17]
$KMnO_4$ modified carbon	7.8	15.9	20	3 h	2	[29]
Calcined Zn/Al hydrotalcite like compound	8.78	13.43	10	4 h	6	[30]
Chitosan-based mesoporous alumina	–	2.22	–	24 h	3–9	[31]
Nano-hydroxyapatite Biogenic apatite	–	4.57 4.99	3–80	100 min	5–6	[10]
Treated biogenic apatite		6.84				
Geogenic apatite		0.014				
ATCP	6	13.54	30–60	90 min	6.6–6.9	This study

where C_o is the initial F concentration and b is Langmuir isotherm constant. The adsorption process as a function of R_L may be described as

$R_L>1$ unfavorable
$R_L = 1$ linear
$0<R_L<1$ favorable
$R_L = 0$ irreversible

R_L values calculated from the present system are presented in Table 2. The R_L values lying between 0 and 1 indicate the favorable conditions for adsorption at all the temperatures studied.

Contrarily to Langmuir, Freundlich isotherm was based on the assumption that the adsorption occurs on heterogeneous sites with nonuniform distribution of energy level. The Freundlich describes reversible adsorption and is not restricted to the formation of monolayer.

The nonlinear form of Freundlich isotherm is:

$$q_e = K_F C_e^{\frac{1}{n}} \tag{20}$$

where C_e is the equilibrium fluoride concentration (mg L^{-1}), q_e is the amount adsorbed per unit mass of the adsorbent at equilibrium (mg g^{-1}), K_L is the empirical constant of Freundlich isotherm (L mg^{-1}), and n is the empirical parameter related to the intensity of adsorption. Values of 1/n are lying between 0.1 and 1.0, and the n values lying in the range of 1–10 confirm the favorable conditions for adsorption [33]. The Freundlich model contents K_L and n are calculated (Fig. 6) and listed in Table 3.

The Temkin isotherm model assumes that the adsorption energy decreases linearly with the surface coverage due to adsorbent–adsorbate interactions. The nonlinear form of Temkin isotherm is:

$$q_e = RT/B_T \ln A_T C_e \tag{21}$$

where B_T is the Temkin constant related to the heat of sorption (J mol^1), A_T is the Temkin isotherm constant (L mg^1), R is the gas constant (8.314 J mol^1 K^1), and T is

Table 2
Dimensionless separation factor (R_L) values for fluoride sorption by ATCP at different temperatures

Fluoride concentration (mg L^{-1})	Temperature		
	25°C	30°C	40°C
30	0.16	0.15	0.13
35	0.14	0.13	0.11
40	0.12	0.12	0.10
45	0.11	0.10	0.09
50	0.10	0.10	0.08
60	0.08	0.08	0.07

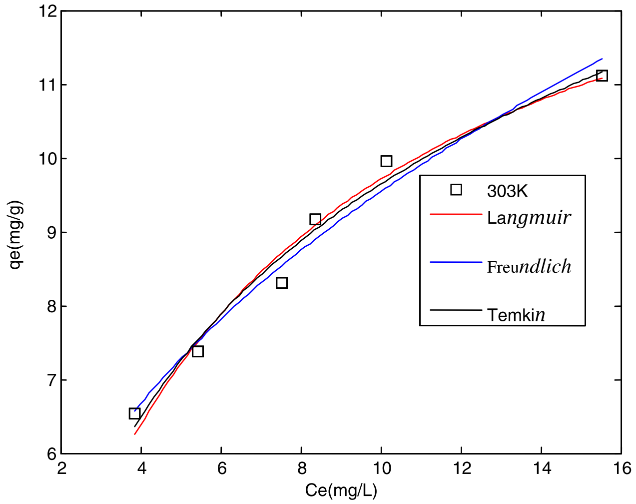

Fig. 6. Isotherms obtained using the nonlinear method for the adsorption of fluoride onto ATCP at a temperature of 303 K. (adsorbent dose 0.2 g, initial concentration 30–60 mg L^1, contact time 90 min, and pH (6.8–6.9)).

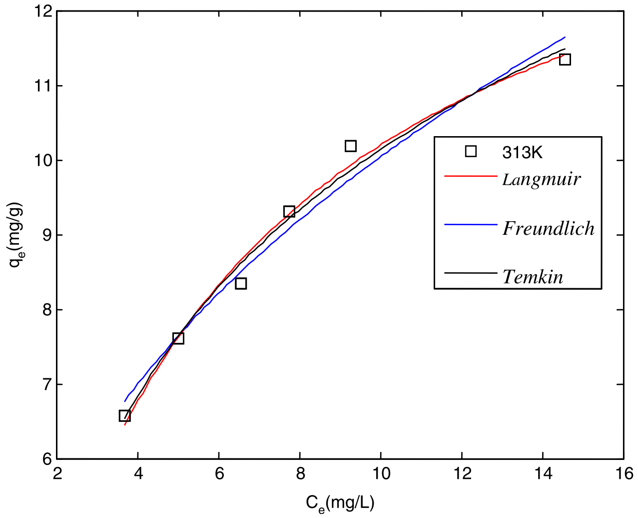

Fig. 7. Isotherms obtained using the nonlinear method for the adsorption of fluoride onto ATCP at a temperature of 313 K. (adsorbent dose 0.2 g, initial concentration 30–60 mg L^1, contact time 90 min, and pH (6.8–6.9)).

the absolute temperature (K). The parameters of Temkin model are determined (Fig. 7) and are listed in Table 3.

The Dubinin–Radushkevick (D–R) isotherm was used to determine the nature of the adsorption process viz. physisorption or chemisorption. The nonlinear form of this model is expressed by:

$$q_e = Q_{D-R} \exp\left(-\alpha\varepsilon^2\right) \tag{22}$$

where q_e is the amount of fluoride ions adsorbed per unit dosage of the adsorbent (mol/g), Q_{D-R} the monolayer capacity, and α is the activity coefficient related to mean sorption energy and ε is the Polanyi potential described as

$$\varepsilon = RT\ln(1 + 1/Ce) \tag{23}$$

The mean sorption energy, E (kJ mol^{-1}), can be calculated by using the following equation:

$$E = (2\alpha)^{1/2} \tag{24}$$

A representative plot of D–R isotherm is depicted at Fig. 8. The statistical results along with the isotherm

Table 3
The value of parameters for each isotherm model used in the studies

Models		T (K)		
		298	303	310
Langmuir	b(L mg^{-1})	0.183	0.186	0.194
	Q_m(mg g^{-1})	13.54	14.90	15.42
	R^2	0.960	0.978	0.988
Freundlich	K_f (Lmg^{-1})	3.68	3.872	4.04
	n	2.72	2.552	2.50
	R^2	0.973	0.976	0.973
Temkin	b_t (J mol^1)	811.25	729.403	720.33
	a_t (Lg^{-1})	1.72	1.63	1.65
	R^2	0.969	0.9806	0.986
D–R	E(kJmol^{-1})	11.265	11.18	16.32
	α (mol^2J^{-2})	3.94×10^{-9}	4.00×10^{-9}	3.75×10^{-9}
	R^2	0.974	0.980	0.980

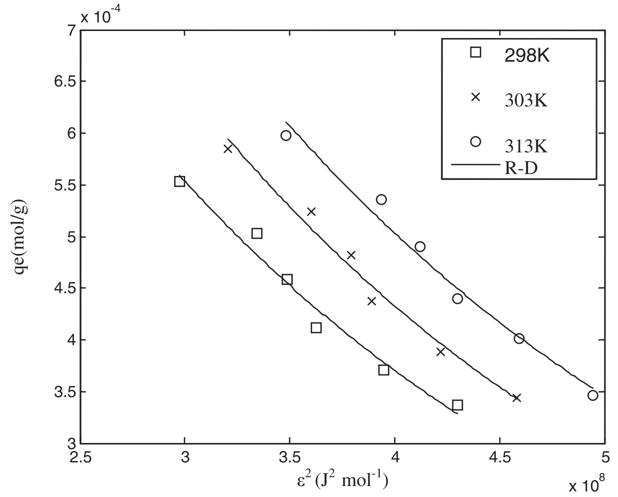

Fig. 8. Plot of D–R isotherm for fluoride adsorption on ATCP (adsorbent dose 0.2 g, initial concentration 30–60 mg L^{1}, contact time 90 min, and initial solution pH (6.8–6.8)).

constants are also given in Table 3. It can be seen that the mean sorption energy (E) was evaluated as 11.18–16.32 kJ mol^{-1} for the adsorption of fluoride at temperature ranging from 298 to 313 K. According to the literature [34], the E value ranges from 1.0 to 8.0 kJ mol^{-1} for physical adsorption and from 9.0 to 16.0 kJ mol^{-1} for chemical ion-exchange adsorption. Therefore, these results indicate that the adsorption of fluoride onto ATCP may be attributed to chemical ion-exchange mechanism.

The calculated results of the Langmuir, Freundlich, Temkin, and Dubinin–Radushkevick isotherm constants are given in Table 3. It is found that the adsorption of fluoride on the ATCP correlated well with the Langmuir, Freundlich, Temkin, and Dubinin–Radushkevick equations under the concentration range studied indicating possibility simultaneous validity of multiple isotherms.

3.5. Thermodynamic investigations

The thermodynamic parameters for the adsorption process in solution have been calculated using the following standard thermodynamic relations [35,36]:

$$\Delta G^{\circ} = -RT\ Lnb \tag{25}$$

$$\Delta G^{\circ} = \Delta H^{\circ} - T\Delta S^{\circ} \tag{26}$$

where ΔG° is the standard free energy change (kJ/mol), ΔH° is the standard enthalpy change (kJ/mol), ΔS° is standard entropy change (kJ $mol^{-1}\,K^{-1}$), b(L/mol) is the adsorption equilibrium constant obtained from Langmuir isotherm, T is the temperature in Kelvin, and R is the universal gas constant (8.314 J $mol^{1}\,K^{1}$).

The values of ΔH° and ΔS° can be obtained from the slope and intercept of a plot of ΔG° against T (Fig. 9). The calculated thermodynamic parameters are presented in Table 4.

The negative values of ΔG° confirm the spontaneous nature of sorption of fluoride by ATCP. The value of ΔG° becomes more negative with increasing temperature. This shows that the removal process is favored by an increase in temperature. The positive value of ΔH° showed that the adsorption process is endothermic in nature. Positive values of ΔH° were also reported for the sorption of fluoride by nanohydroxyapatite/chitosan [11], Brushite [14], and calcined magnesia/pullulan composite [37].

The positive value of ΔS° shows increased randomness at the solid-solution interface during adsorption.

3.6. Adsorption kinetics studies

To investigate the mechanism of adsorption, the pseudo-first-order, pseudo-second-order, and intraparticle diffusion were studied. The adsorption kinetics was studied with initial fluoride concentrations (30, 40, and 50 mg L^{1}) and temperatures (293,303, and 313 K). The uptake of fluoride on adsorbents occurred rapidly and reached equilibrium with in 90 min.

The kinetics of fluoride adsorption on the ATCP was determined by using three different kinetic models, which are pseudo-first-order [38], pseudo-second-order [39], and intra-particle diffusion [40] models.

The nonlinearized form of pseudo-first-order rate equation is given as

$$q_t = q_e(1 - \exp(-k_1 t)) \tag{27}$$

where q_e is the amount of solute on the surface of the sorbent at equilibrium, (mg g^{-1}); q_t is the amount of solute on the surface of the sorbent at time t, (mg g^{-1}); k_1 is the equilibrium rate constant of pseudo-first sorption, (L min^{-1}).

The pseudo-first-order rate constant (k_1) and theoretical equilibrium adsorption capacities $q_e(cal)$ are

Table 4
Thermodynamic parameters for fluoride adsorption by ATCP

T(K)	ΔG° (kJ mol^{-1})	ΔH° (kJ mol^{-1})	ΔS° (kJ $mol^{-1}\,K^{-1}$)
298	−20.20	2.88	0.774
303	−20.58		
313	−21.36		

given in Tables 5 and 6. The value of coefficient of determination is 0.742–0.903. Therefore, we can say that the adsorption of fluoride on the ATCP does not follow the pseudo-first-order kinetic model.

The pseudo-second-order rate equation is expressed as

$$q_t = \frac{k_2 q_e^2 t}{1 + k_2 q_e t} \tag{28}$$

The graph of q_t vs. t (Figs. 10 and 11) for the non-linear pseudo-second-order model has been plotted, and the second-order rate constant k_2 and maximum adsorption capacity q_e have been calculated, respectively (Tables 5 and 6). The correlation coefficient value is high, and the equilibrium adsorption capacity q_e (cal) determined by using the second-order model is nearly the experimentally determined equilibrium adsorption capacity q_e (exp) (Tables 5 and 6).

According to the intra-particle diffusion model proposed by Weber and Morris, the initial rate of intra-particle diffusion can be calculated by plotting q_t against t

$$q_e = k_p t^{1/2} + C \tag{29}$$

where q_t is amount of solute on the surface of the sorbent at time t, (mg g^1), k_p is the intra-particle rate constant (mg g^1 min$^{0.5}$), t is the time (min), and C (mg g^1) is a constant that gives an idea about the thickness of the boundary layer.

The intra-particle rate constant k_p and C parameters obtained from the plots of q_t vs. t for the intra-particle diffusion model are given in Tables 5 and 6. The value of C obtained from intra-particle diffusion model is not zero and the coefficient of determination ($R^2 = 0.585$–0.777) is not satisfactory, indicating that the intra-particle diffusion may not be the controlling factor in determining the kinetics of the process.

Table 5
The kinetic parameters obtained for fluoride adsorption on ATCP at different concentrations

Kinetic equations	Parameters	30 mg L^{-1}	40 mg L^{-1}	50 mg L^{-1}
Pseudo-second-order	k_2 (g mg^{-1} min^{-1})	0.048	0.073	0.087
	$q_e(cal)$ (mg g^{-1})	6.44	7.82	9.52
	$q_e(ex)$ (mg g^{-1})	6.39	7.81	9.50
	R^2	0.966	0.922	0.967
Pseudo-first-order	k_1 (min^{-1})	0.205	0.327	0.467
	$q_e(ca)l$ (mg g^{-1})	6.00	7.36	8.97
	$q_e(ex)$ (mg g^{-1})	6.39	7.81	9.50
	R^2	0.887	0.742	0.782
Intra-particle diffusion	k_p (g mg^{-1} min$^{0.5}$)	0.319	0.295	0.284
	C (mg g^{-1})	3.21	4.97	6.80
	R^2	0.729	0.665	0.585

Table 6
The kinetic parameters obtained for fluoride adsorption on ATCP at different temperatures

Kinetic equations	Parameters	293 K	303 K	313 K
Pseudo-second-order	k_2 (g mg^{-1} min^{-1})	0.044	0.0487	0.0570
	q_e(cal) (mg g^{-1})	5.1036	6.444	7.1076
	$q_e(ex)$ (mg g^{-1})	4.96	6.39	7.20
	R^2	0.9701	0.9662	0.9711
Pseudo-first-order	k_1 (min^{-1})	0.161	0.205	0.248
	$q_e(cal)$ (mg g^{-1})	4.684	6.005	6.668
	$q_e(ex)$ (mg g^{-1})	4.96	6.39	7.2
	R^2	0.903	0.887	0.880
Intra-particle diffusion	k_p (g mg^{-1} min$^{0.5}$)	0.2951	0.0.3191	0.3135
	C (mg g^{-1})	2.068	3.2137	3.9843
	R^2	0.777	0.7299	0.6887

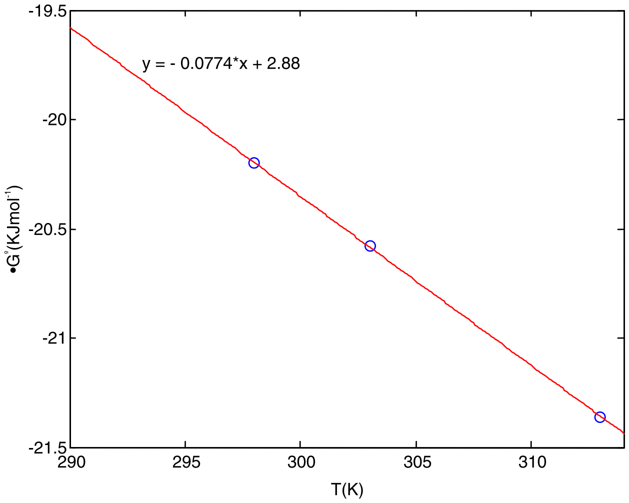

Fig. 9. Van’t Hoff plot.

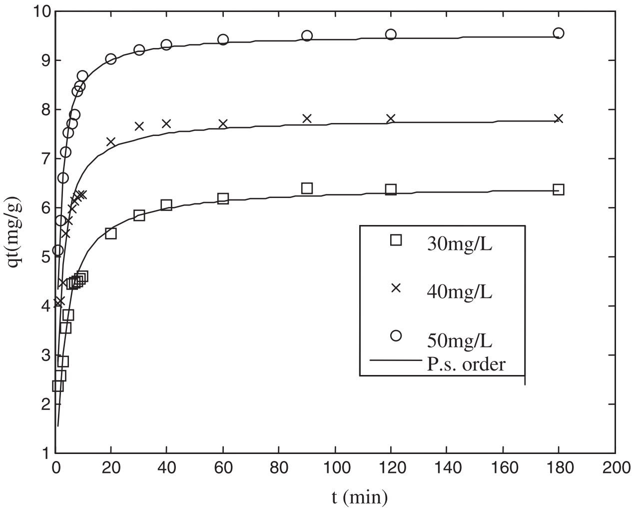

Fig. 10. Pseudo-second-order plots of ATCP (adsorbent dose 0.2 g, T = 303 K and initial solution pH).

As a result, we can say that the pseudo-second-order kinetic model suggested a good correlation for the adsorption of fluoride on the ATCP contrast to the pseudo-first-order model and intra-particle diffusion model, so pseudo-second-order model is suitable for modeling the adsorption of fluoride on the ATCP. This finding suggests that the rate-limiting step of the adsorption system may be chemisorption.

Similar results were also reported for the removal of fluoride onto hydroxyapatite [13], nanosized hydroxyapatite by low-molecular-weight organic acids [41], and various apatite materials [10].

3.7. Desorption experiments

The recycling of an adsorbent is most important aspect for an economical technology. For this purpose, first, the fluoride-adsorbed ATCP is generated by adsorbing 30 mg L^{-1} fluoride solution on 0.2 g ATCP at pH 6.8 and at temperature 30˚C. After the equilibration, the residue was filtered and the filtrate was measured for fluoride content. Then the adsorbent was transferred to 50 mL of distilled water with varying pH (4, 11.75, and12.75). The solutions were then shaken for about 60 min after which the fluoride amount desorbed into the solution was determined to calculate removal extent (percent). It was observed that at pH 4, 11.75, and 12.75 around 2, 23, and 88% desorption efficiencies were found, respectively.

3.8. Treatment of underground water

The defluoridation efficiency of ATCP was experienced with the sample water collected from Youssoufia (Morroco) containing 4.4 mg L^{-1} fluoride. The chemical analysis of the water before and after treatment was presented in Table 7. About 0.2 g of adsorbent was added to 100 mL of fluoride water sample and the contents were shaken (300 rpm) with constant time (90 min) at room temperature. The percentage of fluoride elimination is 100%.

3.9. Effect of the presence of co-existing ions

The drinking water contains several common other anions, viz. nitrate, sulfate, and chloride, which can compete with fluoride ions during the adsorption process for the active sites on the ATCP. Hence, the effect of these competitive ions on the uptake of fluoride ions should be studied. The initial concentration of fluoride was fixed at 30 mg L^{-1} while the initial concentration of other anions varied from 100 to 500 mg L^{-1}.

Fig. 12 shows the effect of various coexisting ions of different concentrations on fluoride sorption by ATCP. Except HCO3, all other coexisting ions (CL^-, NO_3^-, and SO_4^{2-}) have shown negligible effect on fluoride sorption. The reduction in fluoride removal

Table 7
Water quality parameters before and after treatment

Water quality parameters	Before treatment	After treatment
pH	7.75	7.18
F^-	4.4	0
Cl^-	200	196
$SO_4{}^{2-}$	180	174.8
$NO_3{}^-$	30	28
$HCO_3{}^-$	300	289.6

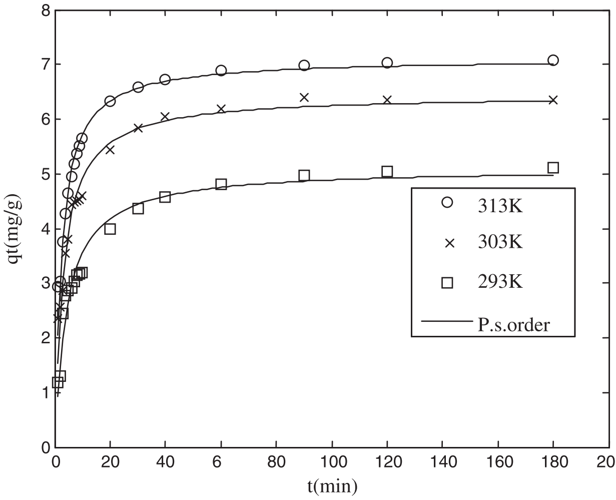

Fig. 11. Pseudo-second-order plots of ATCP (adsorbent dose 0.2 g, initial concentration $30\,\text{mg}\,\text{L}^1$, and initial solution pH).

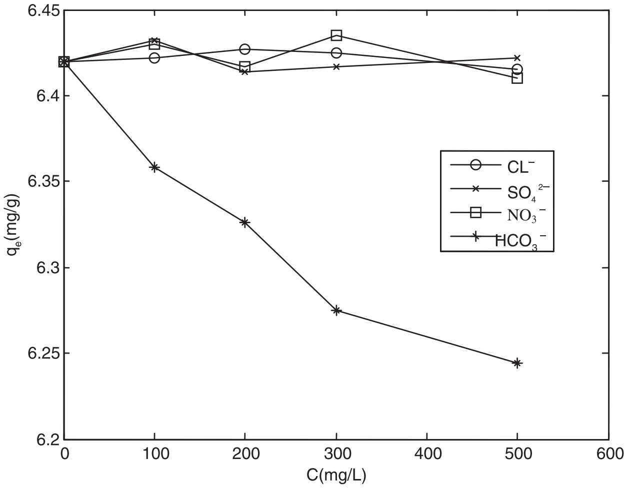

Fig. 12. Effect of presence of co-ions on fluoride adsorption.

observed by the presence of HCO_3^- may be due to competition from this ion for active sorption site or due to the change in pH or combination of these two.

4. Conclusions

This study was demonstrated that the ATCP can be used as an adsorbent for batch adsorption of F^- ions from aqueous solution under different conditions. Experimental data were shown a good fit with the Langmuir, Freundlich, Temkin, and Dubinin–Radushkevick. Thermodynamic analysis was shown that the adsorption process was endothermic and spontaneous in nature. The kinetic study was indicated that the adsorption of fluoride is very rapid, and the equilibrium reached within 90 min. The adsorption data was modeled using the pseudo-first, pseudo-second-order kinetic, and intra-particle diffusion equations. It was shown that the pseudo-second-order kinetic best describes the sorption kinetic. The presence of CL^-, SO_4^{2-}, and NO_3^- lead to negligible change in defluoridation capacity, however, the presence of HCO_3^- decreased the defluoridation capacity. It was observed that at pH 4, 11.75, and 12.75 around 2, 23, and 88% desorption efficiencies were found, respectively.

References

[1] WHO, Fluoride in Drinking-Water by J. Fawell, K. Bailey, J. Chilton, E. Dahi, L. Fewtrell and Y. Magara. ISBN: 1900222965. Published by IWA Publishing, London.

[2] W.K.N. Moturi, M.P. Tole, T.C. Davies, The contribution of drinking water towards dental fluorosis: A case study of Njoro division, Nakuru district, Kenya, Environ. Geochem. Health 24 (2000) 123.

[3] A. Bhatnagar, E. Kumar, M. Sillanpää, Fluoride removal from water by adsorption, Chem. Eng. J 171 (2011) 811.

[4] K. Muthukumaran, N. Balasubramanian, T.V. Ramakrishna, Removal of fluoride by chemically activated carbon, Ind. J. Environ. Protect. 15 (1955) 514.

[5] X. Fan, D.J. Parker, M.D. Smith, Adsorption kinetics of fluoride on low cost materials, Water Res 37 (2003) 4929.

[6] K.K. Pant, S. Ghorai, Equilibrium, kinetics and breakthrough studies for adsorption of fluoride on activated alumina, Sep. Purif. Technol. 42 (2005) 265.

[7] B. Kemer, D. Ozdes, A. Gundogdu, V.N. Bulut, C. Duran, M. Soylak, Removal of fluoride ions from aqueous solution by waste mud, J. Hazard. Mater. 186 (2009) 888.

[8] A. Tor, Removal of fluoride from an aqueous solution by using montmorillonite, Desalination 201 (2006) 267.

[9] M.G. Sujana, H.K. Pradhan, S. Anand, Studies on sorption of some geomaterials for fluoride removal from aqueous solutions, J. Hazard. Mater. 161 (2009) 120.

[10] S. Gao, J. Cui, Z. Wei, Study on the fluoride adsorption of various apatite materials in aqueous solution, J. Flu. Chem. 130 (2009) 1035.

[11] C. Sairam Sundaram, N. Viswanathan, S. Meenakshi, Defluoridation chemistry of synthetic hydroxyapatite at nano scale: Equilibrium and kinetic studies, J. Hazard. 155 (2008) 206.

[12] W. Liang, L. Zhan, L. Piao, C. Russel, Fluoride removal performance of glass derived hydroxyapatite, Mater. Res. Bull. 46 (2011) 205.

[13] M. Mourabet, A. El Rhilassi, H. El Boujaady, M. Bennani-Ziatni, R. El Hamri, A. Taitai, Removal of fluoride from aqueous solution by adsorption on hydroxyapatite (HAp) using response surface, JS Chem. Soc. doi:10.1016/j.jscs.2012.03.003.

[14] M. Mourabet, H. El Boujaady, A. El Rhilassi, H. Ramdane, M. Bennani-Ziatni, R. El Hamri, A. Taitai, Defluoridation of water using brushite: Equilibrium, kinetic and thermodynamic studies, Desalination 278 (2011) 1.

[15] J. C. Heughebaert, PhD Thesis status, I.N.P, Toulouse, (1977).

[16] M. Mourabet, A. El Rhilassi, H. El Boujaady, M. Bennani-Ziatni, R. El Hamri, A. Taitai, Removal of fluoride from aqueous solution by adsorption on Apatitic tricalcium phosphate using Box–Behnken design and desirability function, Appl. Surf. Sci. 258 (2012) 4402.

[17] S.M. Maliyekkal, S. Shukla, L. Philip, I.M. Nambi, Enhanced fluoride removal from drinking water by magnesia-amended activated alumina granules, Chem. Eng. J. 140 (2008) 183.

[18] Y. Li, P. Zhang, Q. Du, X. Peng, T. Liu, Z. Wang, Y. Xia, W. Zhang, K. Wang, H. Zhu Dehai, Adsorption of fluoride from aqueous solution by graphene, J. Coll. Inter. Sci. 363 (2011) 348.

[19] M.J. Reyes, M.S. Ríos, Sorption behavior of fluoride ions from aqueous solutions by hydroxyapatite, J. Hazard. Mater. 180 (2010) 297.

[20] N. Chen, Z. Zhang, C. Feng, M. Li, D. Zhu, N. Sugiura, Studies on fluoride adsorption of iron-impregnated granular ceramics from aqueous solution, Mater. Chem. Physics 125 (2011) 293.

[21] M.G. Sujana, S. Anand, Fluoride removal studies from contaminated ground water by using bauxite, Desalination 267 (2011) 222.

[22] J. Ma, J. Qi, C. Yao, B. Cui, T. Zhang, D. Li, A novel bentonite-based adsorbent for anionic pollutant removal from water, Chem. Eng. J. 200 (2012) 97.

[23] I. Langmuir, The adsorption of gases on plane surfaces of glass, mica and platinum, J. Am. Chem. Soc. 40 (1918) 1361.

[24] H.M.F. Freundlich, Über die adsorption in lösungen [Over the adsorption in solution]. J. Phys. Chem. 57 (1906) 385.

[25] M.J. Temkin, V. Pyzhev, Recent modification of Langmuir isotherms, Acta Physiochim. URSS 12 (1940) 217.

[26] M.M. Dubinin, L.V. Radushkevich, Equation of the characteristic curve of activated charcoal, Chem. Zentr. 1 (1947) 875.

[27] X. Dou, Y. Zhang, H. Wang, T. Wang, Y. Wang, Performance of granular zirconium-iron oxide in the removal of fluoride from drinking water, Water Res., in press, doi:10.1016/j.watres.2011.04.002.

[28] S. Jagtap, D. Thakre, S. Wanjari, S. Kamble, N. Labhsetwar, S. Rayalu, New modified chitosan-based adsorbent for defluoridation of water, J. Colloid. Interface Sci. 332 (2009) 280.

[29] A.A.M. Daifullah, S.M. Yakout, S.A. Elreefy, Adsorption of fluoride in aqueous solutions using $KMnO_4$-modified activated carbon derived from steam pyrolysis of rice straw, J Hazard. Mater. 14 (2007) 633.

[30] S. Jagtap, M.K.N. Yenkie, N. Labhsetwar, S. Rayalu, Defluoridation of drinking water using chitosan based mesoporous alumina, Microporous Mesoporous Mater. 142 (2001) 454.

[31] D. Thakre, S. Jagtap, N. Sakhare, N. Labhsetwar, S. Meshram, S. Rayalu, Chitosan based mesoporous Ti-Al binary metal oxide supported beads for defluoridation of water, Chem. Eng. J. 158 (2010) 315.

[32] T.W. Weber, R.K. Chakravarty, Pore and solid diffusion models for fixed bed adsorbers, Am. Inst. Chem. Eng. J. 20 (1974) 228.

[33] K.R. Hall, L.C. Eagleton, A. Acrivos, T. Vermeulen, Pore- and solid-diffusion kinetics in fixed-bed adsorption under constant-pattern conditions, Ind. Eng. Chem. Fund. 5 (1966) 212.

[34] F. Helfferich, Ion Exchange, McGraw-Hill, New York, NY, 1962.

[35] Y.S. Ho, Isotherms for the sorption of lead onto peat: Comparison of linear and non-linear methods, P. J. Env. Studies 15 (2006) 81.

[36] Z.A. Al-Anber, M.A.D. Matouq, Batch adsorption of cadmium ions from aqueous solution by means of olive cake, J. Hazard. Mater. 151 (2008) 194.

[37] J. Kang, B. Li, J. Song, D. Li, J. Yang, W. Zhan, D. Liu, Defluoridation of water using calcined magnesia/pullulan composite, Chem. Eng. J. 166 (2010) 765.

[38] S. Lagergren, Zur theorie der sogenannten adsorption gelo ster stoffe [About the theory of so-called adsorption of soluble substances], K. Sven. Vetenskapsakad. Handl. 24 (1898) 1.

[39] Y.S. Ho, G. McKay, Pseudo-second order model for sorption processes, Proc Biochem 34 (1999) 451.

[40] W.J. Weber, J.C. Morris, Equilibria and capacities for adsorption on carbon, J. San. Eng. Div. 90 (1964) 79.

[41] Y. Wang, N. Chen, W. Wei, J. Cui, Z. Wei, Enhanced adsorption of fluoride from aqueous solution onto nanosized hydroxyapatite by low-molecular-weight organic acids, Desalination 276 (2011) 161.